CAPACITY LOSS ESTIMATION FOR LI-ION BATTERIES BASED ON A SEMI-EMPIRICAL MODEL

*Mohammed Rabah, Eero Immonen, and Sajad Shahsavari
Computational Engineering and Analysis (COMEA)
Turku University of Applied Sciences
20520 Turku, Finland
Email: *mohamed.rabah@turkuamk.fi

Mohammad-Hashem Haghbayan
Department of Future Technologies
University of Turku (UTU)
20500 Turku, Finland

Kirill Murashko
Department of Environmental and Biologic Science
University of Eastern Finland
70211 Kuopio, Finland

Paula Immonen
Laboratory of Electrical Engineering
LUT University
53850 Lappeenranta, Finland

Keywords

SEM (Semi-Empirical Model), LIBs (Li-ion batteries), C_{loss} (Capacity Loss), Cycling Aging, Calendar Aging.

ABSTRACT

Understanding battery capacity degradation is instrumental for designing modern electric vehicles. In this paper, a Semi-Empirical Model for predicting the Capacity Loss of Lithium-ion batteries during Cycling and Calendar Aging is developed. In order to predict the Capacity Loss with a high accuracy, battery operation data from different test conditions and different Lithium-ion batteries chemistries were obtained from literature for parameter optimization (fitting). The obtained models were then compared to experimental data for validation. Our results show that the average error between the estimated Capacity Loss and measured Capacity Loss is less than 1.5% during Cycling Aging, and less than 2% during Calendar Aging. An electric mining dumper, with simulated duty cycle data, is considered as an application example.

INTRODUCTION

The transport sector is one of the largest global emitters of carbon dioxide (CO_2), accounting for about 22% of the total emission (Kluschke et al., 2019). Electric cars have proven to be an efficient way of reducing these emissions in *passenger transport*, but electrification of *heavy-duty vehicles* (e.g. trucks, forest harvesters and mining dumpers) is more challenging, mainly due to limitations in battery technology. Among others, Liimatainen et al. (2019) concluded that battery electric trucks have not been a viable option to replace traditional diesel-powered ones because of the high energy requirements and low energy density of batteries. Furthermore, the absence of charging facilities in off-road conditions may render electrification of forest harvesters impractical. On the other hand, heavy-duty vehicles are typically tailored for a specific application niche, and their production batches are much smaller than those for passenger cars, which means that application-specific design optimization is both necessary and can also have a significant effect on the vehicle performance — and thus on business profitability. At the heart of this design optimization is an understanding of the performance of lithium-ion (Li-ion) batteries.

One major difference between internal combustion engine vehicles (ICEV) and battery electric vehicles (BEV) is that the energy system in the latter degrades during use. While the performance of a diesel engine remains largely unaffected by repeated refuels and use, this is not the case for Li-ion batteries (LIBs): The capacity of LIBs decreases in both repeated cycling and storage. Moreover, the LIB degradation process depends on the battery chemistry and the way (or path) of usage. Dubarry and Devie (2018) concluded that the LIB cell temperature history had the strongest impact on degradation followed by the C-rate (i.e. charge/discharge current) and the state of charge (SoC). Also, they found that LIBs lose capacity faster at low SoCs during calendar aging and under small SoC swings while under cycling.

It is obvious from the above discussion that design optimization for heavy-duty battery electric vehicles (HDBEV) must address battery degradation. The upshot is that, in contrast to passenger cars, since a HDBEV is designed for a specific application, the typical usage conditions — including temperature, SoC and C-rate — can often be estimated with more accuracy during design. Battery system design optimization for HDBEVs thus requires parametric mathematical models of battery aging, estimated from real-world cycling and storage tests. The purpose of this article is to address this concern.

In this article, a Semi-Empirical Model (SEM) is proposed for estimating the capacity loss (C_{loss}) for different LIB chemistries during cycling and calendar aging. The model is developed based on the effect of four different parameters, namely temperature, time, depth of discharge, and C-rate current. The model is able to estimate the C_{loss} of LIBs with a high accuracy and low computation complexity compared to the other models. This model can be used for optimizing LIB systems for different chemistries throughout their lifetime

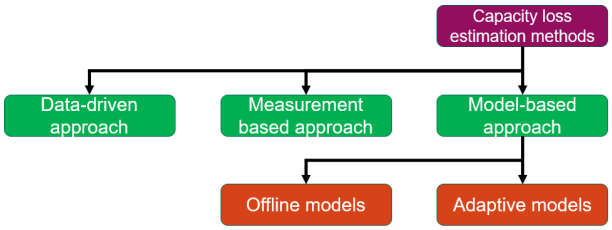

Figure 1: Capacity Loss Estimation methods.

in realistic operation conditions. The contribution of this article is elaborated in the next section.

RELATED WORK

LIB degradation is usually measured by C_{loss}. It reflects the ability of the LIB to store and to supply energy relative to its initial conditions, considering the energy and power requirements of the application (Berecibar et al., 2016). Many different methods for the C_{loss} estimation were presented in recent years and in general they can be divided into three approaches, which are shown in Figure 1.

The measurement based methods by themselves cannot be used for the estimation of the C_{loss} during design of the battery system as these methods requires the analysis of the measured data during operation of the LIB.

The data-driven approach includes methods, where the previously collected information about operation of the LIB is used to find the dependency between the collected information and C_{loss}. Different algorithms such as Support Vector Regression algorithm (Liu et al., 2020), Fuzzy logic (Yang et al., 2020) and Neural Networks (Naha et al., 2020) were investigated for C_{loss} estimation. These methods allows to estimate the C_{loss} with good accuracy in case of the availability of a sufficient amount of previously collected data. However, these methods are computationally intensive and are sensitive to the size and quality of the experimental dataset applied during the training, which are not always available.

The model-based approach (Cacciato et al., 2016) may yield better results for the C_{loss} estimation in case of the low amount of the experimental data. It can be done by applying a model, which should describe the processes occurring in the LIBs. Such models can be used offline and they directly provide the required information on the C_{loss} — or the required information can be obtained during comparison of the calculated and measured data in real time. If a very high accuracy for the C_{loss} estimate is needed, the second type of the battery model, so called adaptive model (Cen & Kubiak, 2020), is often recommended in the literature. The adjustment of the adaptive model parameters and C_{loss} estimation after comparison with measured data can be done by using such algorithms as Kalman Filter, Particle filter, Sliding mode observer etc. As it was reported by (Andre et al., 2013), the use of the adaptive models allows to estimate C_{loss} and State of Charge (SoC) simultaneously with estimation error under 1%.

Despite the high accuracy of the C_{loss} estimation, a high computational complexity may limit the applicability of the adaptive models during battery system design where high accuracy is not always necessary. In this case, offline models such as SEM (Singh et al., 2019) may be more useful as they may estimate the C_{loss} with acceptable uncertainty in case of the lack of the experimental data and they have low computation complexity. In the SEM approach, one attempts to identify a (simple) parametric function that describes the capacity reduction, through parametric optimization.

The applicability of the SEM approach for the C_{loss} estimation during storage (Grolleau et al., 2014) and cycling (Bocca et al., 2015) were widely shown for different LIBs. However, the presented models were usually verified for the same LIBs, from which the SEMs were created and the use of the presented algorithms for the creation of the SEMs for other type of the LIBs is not well discussed. Therefore, the research work described in the present article focused on the analysis of the applicability of the commonly used approach for the creation of the SEMs of different LIBs at different operation conditions.

SEM SPECIFICATIONS

In this article the most commonly used models, which can estimate the capacity loss C_{loss} of the LIBs during Calendar Aging C_{loss}^{cal} and Cycling Aging C_{loss}^{cyc} are analysed. These semi-empirical models were previously used for the modeling of the C_{loss} in LFP cells (Wang et al., 2011), NMC cells (Schmalstieg, Käbitz, Ecker, & Sauer, 2014), NCA cells (Petit, Prada, & Sauvant-Moynot, 2016) and they are briefly described below.

Calendar Aging

The two main factors that affects the Calendar Aging are the T and SoC. The general equation for the Calendar Aging estimation can be presented as:

$$C_{loss}^{cal} = B(SoC) \cdot e^{-\frac{E}{R(T-T_{ref})}} \cdot t^z, \qquad (1)$$

where B is the pre-exponential factor that depends on SoC, T is the temperature expressed in K, T_{ref} is the reference temperature also expressed in K and is equal to 298.15, R is the gas constant, E is the activation energy of a reaction, expressed in J/mol, t is the time in days, and z is a constant. The pre-exponential factor B can be presented as:

$$B = a_1 \cdot SoC + a_2 \qquad (2)$$

Where a_1 and a_2 are fitting constants. Equation 1 can be used to estimate the C_{loss} of the LIB during long period storage.

Cycling Aging

For Cycling Aging, the C_{loss} is mainly affected by current I, T and number of cycles N. Furthermore, other parameters do have a margin effect depending on the temperature of the LIB, e.g. depth of discharge DoD,

and the rated capacity. The general equation used to estimate the C_{loss}^{cyc} is as follow:

$$C_{loss}^{cyc} = B_{cyc}(I) \cdot e^{-\frac{E+\alpha\cdot|I|}{R(T-T_{ref})}} \cdot A_h^{z_{cyc}} \quad (3)$$

Where B_{cyc} is a pre-exponential factor which depends on cycling current I, α and z_{cyc} are the fitting coefficients, and A_h is the full used capacity that can be obtained using the following equation:

$$A_h = FCE \cdot C_r = N \cdot DoD \cdot C_r \quad (4)$$

Where FCE is the full cycle equivalent, C_r is the rated capacity.

MODEL IDENTIFICATION

The process of model identification is divided into two parts; (a) Data Selection and Fitting, and (b) Model Validation. These two parts are illustrated in Figure 2.

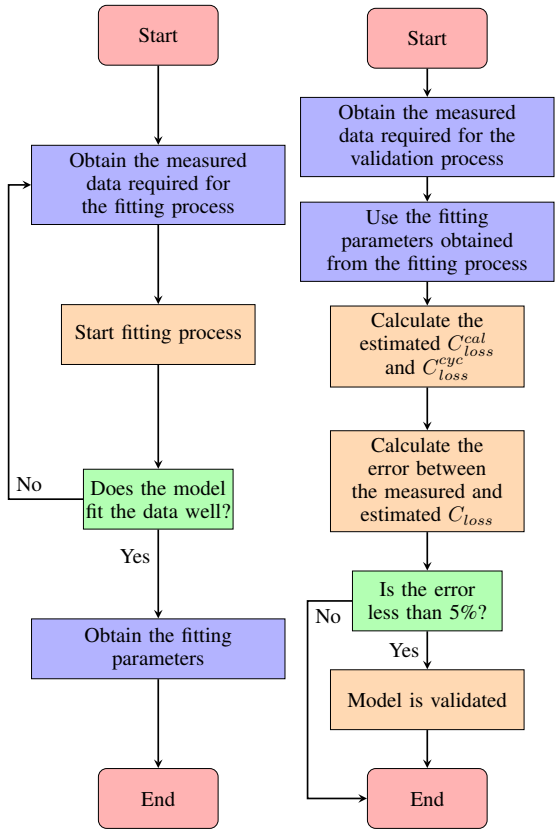

Figure 2: SEM flowchart process; (a) Data Selection and Fitting process, (b) Model Validation process.

Data Selection and Fitting

Figure 2 (a) shows the Flow Chart of the data selection and fitting process. As shown in this Figure, measured data from different references, specifically the C_{loss}^{cal}, C_{loss}^{cyc}, FCE and $Time$ are obtained. Afterwards the fitting process is applied to estimate the value of the fitting parameters. The algorithm used for obtaining the fitting parameters is shown in Algorithm 1. In this algorithm, $Mes\_C_{loss}^{cyc}$ and $Mes\_C_{loss}^{cal}$ are the measured C_{loss} data needed for fitting the model, while $Est\_C_{loss}^{cyc}$ and $Est\_C_{loss}^{cal}$ are the estimated C_{loss} output. In this process, the `fitting` function is using the `fminsearch` from MATLAB which uses a simplex search method (Lagarias et al., 1998) to obtain the estimated data output. In order to decrease the overall error between the measured and the estimated output, the fitting function is proceed in different scenarios, e.g. during a fixed temperature, fixed $DoD = 1 - SoC$, etc., for 1000 iteration in each. For this, several fitting parameters are calculated according to each situation. Once the estimated output reaches the local minimum, the average error is calculated between the estimated output and the measured data. In this case, it's assumed that 5% is when the model does fit the data well. Afterwards, function `fitpar` which uses the `polyfit` from MATLAB is used to generate the fitting parameters based on least square regression. Once these values are calculated, the model validation process is started as shown in Figure 2 (b).

Algorithm 1 Data Selection and Fitting process

Input: $Mes\_C_{loss}^{cyc}$, $Mes\_C_{loss}^{cal}$
Output: $Est\_C_{loss}^{cyc}$, $Est\_C_{loss}^{cal}$,R,a_1,a_2,z,α,z_{cyc},B_{cyc}

Body:

$\mathbf{measured} \leftarrow \{\mathbf{Mes\_C_{loss}^{cyc}}, \mathbf{Mes\_C_{loss}^{cal}}\}$
$\mathbf{estimated} \leftarrow \{\mathbf{Est\_C_{loss}^{cyc}}, \mathbf{Est\_C_{loss}^{cal}}\}$
for i $\leftarrow 1$ **to** 1000 **do**
  $\mathbf{estimated} \leftarrow fitting(\mathbf{measured})$
  if estimated $==$ **localminimum then**
    Stop
  end
end
$\mathbf{error} \leftarrow avg.(\frac{\mathbf{estimated}-\mathbf{measured}}{\mathbf{measured}})$
if error < 0.05 **then**
  $\{\mathbf{E}, \mathbf{R}, \mathbf{a_1}, \mathbf{a_2}, \mathbf{z}, \alpha, \mathbf{z_{cyc}}, \mathbf{B_{cyc}}\} \leftarrow fitpar(\mathbf{estimated})$
end

Algorithm 2 Model Validation process

Input: $NewMeasuredData$
Output: C_{loss}^{cyc}, C_{loss}^{cal}
Parameters: R,a_1,a_2,z,α,z_{cyc},B_{cyc},T_{ref}

Body:

$\{\mathbf{SoC}, \mathbf{T}, \mathbf{I}, \mathbf{t}, \mathbf{N}, \mathbf{period}, \mathbf{C_r}\} \leftarrow \mathbf{NewMeasuredData}$
`// Calculate` C_{loss} `for Cycling Aging`
$\mathbf{cyc.DoD}, \mathbf{cyc.SoC}, \mathbf{ch1}, \mathbf{ch2} \leftarrow$ rainflow($\mathbf{SoC}$);
$\mathbf{cyc.I} \leftarrow avg.\,\mathbf{I}\ from\ \mathbf{ch1}\ \mathbf{to}\ \mathbf{ch2}$;
$\mathbf{cyc.T} \leftarrow avg.\,\mathbf{T}\ from\ \mathbf{ch1}\ \mathbf{to}\ \mathbf{ch2}$;
$\mathbf{C_{loss}^{cyc}} \leftarrow B_{cyc} \cdot e^{-\frac{E+\alpha\cdot|cyc.I|}{R(cyc.T-T_{ref})}} \cdot (NC_r(cyc.DoD))^{z_{cyc}}$
`// Calculate` C_{loss} `for Calendar Aging`
if $\mathbf{I} == 0$ **then**
  $\mathbf{cal.SoC} = avg.\,(\mathbf{SoC})$;
  $\mathbf{cal.T} = avg.\,(\mathbf{T})$;
  $\mathbf{cal.t} = \mathbf{period} * 24 * 3600$;
  $\mathbf{B(SoC)} = \mathbf{a_1} \cdot \mathbf{cal.SoC} + \mathbf{a_2}$;
  $\mathbf{C_{loss}^{cal}} \leftarrow B(SoC) \cdot e^{-\frac{E}{R(cal.T-T_{ref})}} \cdot cal.t^z$
end

Model Validation

In this process, the estimated fitting parameters values are input into Equations (1)-(4), to calculate the C_{loss} during Cycling/Calendar aging, and the output

is compared to a known reference, where the error is calculated between the known C_{loss} and the estimated one. If the error is low (here defined as below 5%), this shows that the model is validated and can be used to estimate the C_{loss} of an experimental LIB.

The method used for calculating the C_{loss} is shown in Algorithm 2. The information about state of charge SoC, temperature T, current I, rated capacity C_r and time between operation cycles is necessary for the C_{loss} calculation t. The loss of the capacity during cycling is calculated from information about N, cycle start time $ch1$ and end time $ch2$, average values of $cyc.DoD$ and $cyc.SoC$ that are calculated from SoC curve by using `Rainflow` algorithm in MATLAB (ASTM E1049-85, 2005). Afterwards, average values of temperature $cyc.T$ and current $cyc.I$. are calculated during a cycle to be used in Equation 3. The calendar C_{loss} is calculated by considering the average state of charge $cal.SoC$ and average temperature $cal.T$ of each long enough period of time when LIBs are not used where there is no current usage during this period.

RESULTS

To test the feasibility of the proposed model, several LIB chemistries should be evaluated. In this work, two different chemistries of LIBs have been chosen; Lithium Iron Phosphate (LFP) and Lithium-Titanate Oxide (LTO). These chemistries are among the primary candidates for modern HDBEV systems.

Lithium-titanate battery (LTO)

Data Selection and Fitting

The measured data that is used for the fitting process is acquired from (Dubarry & Devie, 2018). In his work, he studied the effect of temperature 'T', SoC swing range '$\triangle SoC$', and C-rate 'C' on the battery cells to measure its C_{loss} during 1400 ($1C$ rate) to 4200 ($3C$ rate) full cycle equivalent as demonstrated in Figure 3(a). Likewise, he studied the effect of 'T' and SoC through 61 weeks of Calendar Aging as illustrated in Figure 3(b).

Once the measured data from Figure 6 is extracted, the fitting process is started. The fitting function for the Cycling Aging is proceed in four different scenarios: during a fixed $DoD(40\%)$, fixed temperature (25°C), and fixed C-rate. Figure 4 shows the estimated C_{loss} (dashed line) compared to the measured one (solid line). The average error between the estimated C_{loss} and measured C_{loss} is found to be 0.63% at 50% of FCE and 0.54 at 100% of FCE, except for one point that shows an error of 0.72% during the 4200 FCE that can be found in Figure 4(d) (45/0.7/3).

In the Calendar Aging fitting process, the model has an average error of 0.8% between the estimated C_{loss} (dashed line) and the measured one (solid line), except for the condition T = (55°C), SoC = 5%, as the model does have an average error of 1.4% during this condition.

The results from the literature shows that during Calendar Aging, the LTO tends to degrade faster while the SoC is low compared to higher SoC, in addition to the effect of T. For Cycling Aging, the increase in T and C-rate has significant effect on the LTO chemistry, and the degradation rate is faster when smaller SoC swings $\triangle SoC$ is applied.

Model Validation

In order to test the performance of the proposed model, it needs to be validated and compared to another known measured C_{loss} during cycling and Calendar Aging. For the Cycling Aging, the input data needed for the C_{loss} algorithm is extracted from (Baure & Dubarry, 2020), and the output is compared to the C_{loss} from the same reference. Table 1 and Table 2 first columns show a summary of the extracted data that is required for the Cycling Aging C_{loss}. Furthermore, both tables show the measured C_{loss} in 25/35°C, estimated C_{loss} and the error during 2500 equivalent cycles.

As shown in Table 1, the model does have an average error of 0.46% during Cycling Aging in 25°C, while it does have an average error of 1.39% in 35°C as shown in Table 2.

Table 1: Data validation during Cycling Aging measured in 25°C

Data cycling measured in 25 °C	**Measured Capacity Loss %**	**Estimated Capacity Loss %**	**Error %**
Median SoC = 15%, △SoC = 5%	0.37	0.69	0.32
Median SoC = 50%, △SoC = 5%	0.33	0.69	0.36
Median SoC = 85%, △SoC = 5%	0.33	0.69	0.36
Median SoC = 15%, △SoC = 45%	0.42	1.07	0.65
Median SoC = 50%, △SoC = 45%	0.40	1.07	0.67
Median SoC = 85%, △SoC = 45%	0.48	1.07	0.59
Median SoC = 50%, △SoC = 75%	0.41	0.71	0.30

Table 2: Data validation during Cycling Aging measured in 35°C

Data cycling measured in 35 °C	**Measured Capacity Loss %**	**Estimated Capacity Loss %**	**Error %**
Median SoC = 15%, △SoC = 5%	0.54	1.60	1.06
Median SoC = 50%, △SoC = 5%	0.58	1.60	1.02
Median SoC = 85%, △SoC = 5%	0.54	1.60	1.06
Median SoC = 15%, △SoC = 45%	0.62	2.48	1.86
Median SoC = 50%, △SoC = 45%	0.59	2.48	1.89
Median SoC = 85%, △SoC = 45%	0.70	2.48	1.78
Median SoC = 50%, △SoC = 75%	0.58	1.62	1.04

For the Calendar Aging, the required data is extracted and compared to the measured C_{loss} in (Dubarry et al., 2018). Table 3 shows a summary of the extracted data from this reference. To estimate the C_{loss} per 1 month,

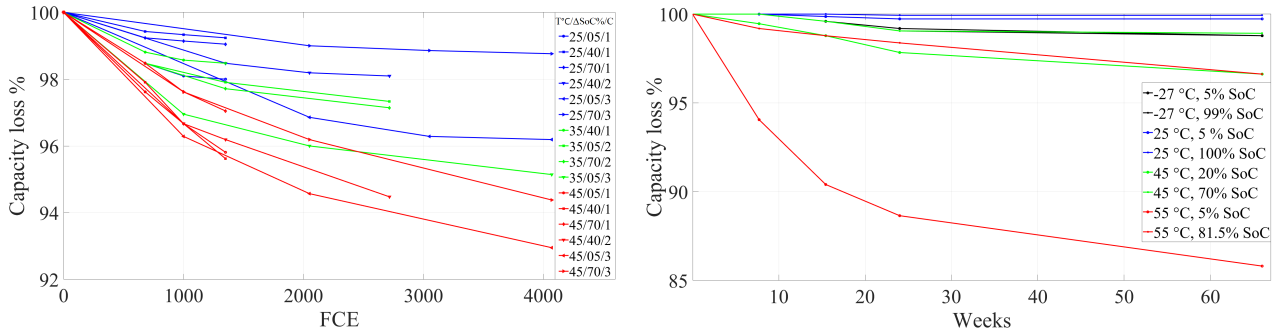

(a) Capacity Loss as a function of FCE

(b) Capacity Loss as a function of storage time

Figure 3: LTO measured Capacity Loss during Cycling and Calendar Aging (Dubarry & Devie, 2018).

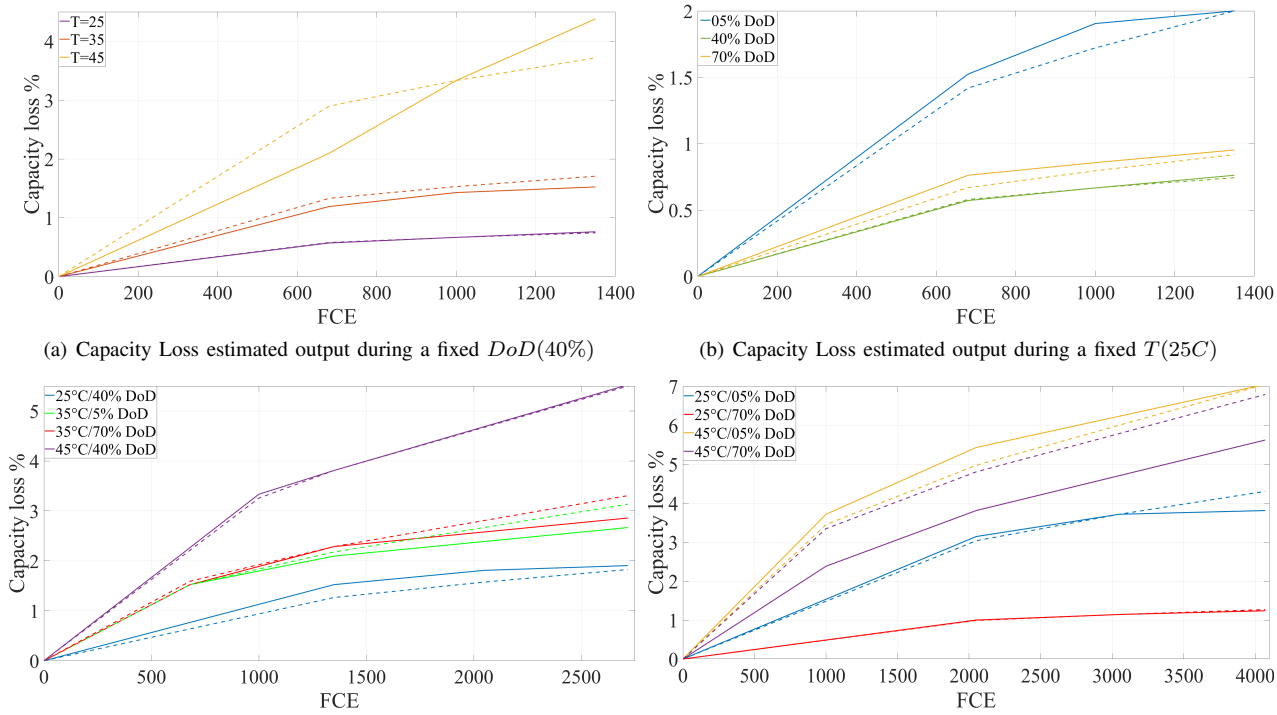

(a) Capacity Loss estimated output during a fixed $DoD(40\%)$

(b) Capacity Loss estimated output during a fixed $T(25C)$

(c) Capacity Loss estimated output during a fixed $C-rate(2C)$

(d) Capacity Loss estimated output during a fixed $C-rate(3C)$

Figure 4: LTO estimated Capacity Loss during Cycling Aging.

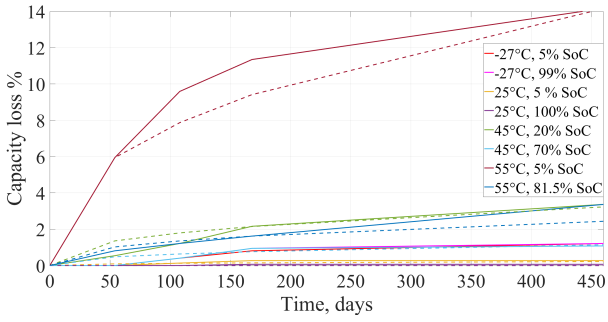

Figure 5: LTO estimated Capacity Loss during Calendar Aging.

`fitlm` from MATLAB is used to fit a linear regression model to obtain this value. Afterwards, the number of days is calculated and used as an input to the developed model. Table 3, 4th column shows the error between the estimated C_{loss} and the measured one. The model does have an average error of 1.98% in Calendar Aging.

Table 3: Data validation during Calendar Aging

Temperature °C	SoC %	Capacity Loss (%/month)	Error %
-27	5	0.28	2.03
-27	99	0.28	1.95
25	50	0.05	0.67
25	100	0.05	0.68
45	20	0.76	2.74
45	70	0.24	1.76
55	5	3.97	3.37
55	81.5	0.73	2.67

Lithium iron phosphate battery (LFP)

Data Selection and Fitting

The measured data required for the fitting process during Cycling Aging is obtained from (Wang et al.,

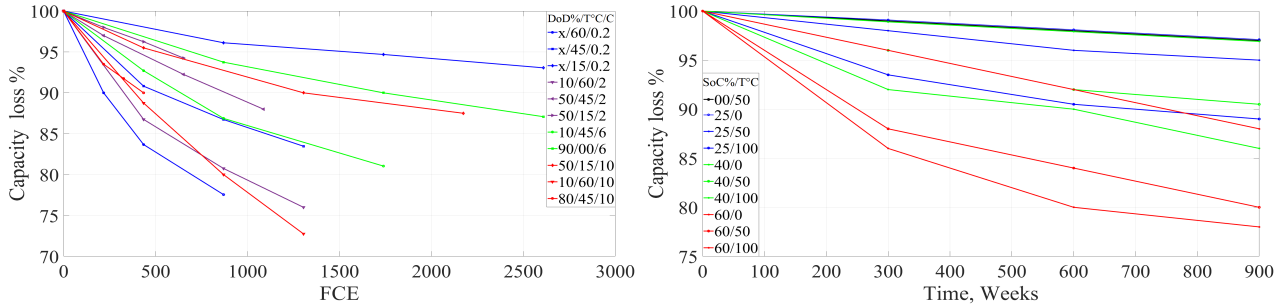

(a) Capacity Loss as a function of FCE (Wang et al., 2011)

(b) Capacity Loss as a function of storage time (Naumann et al., 2018)

Figure 6: LFP measured Capacity Loss during Cycling and Calendar Aging.

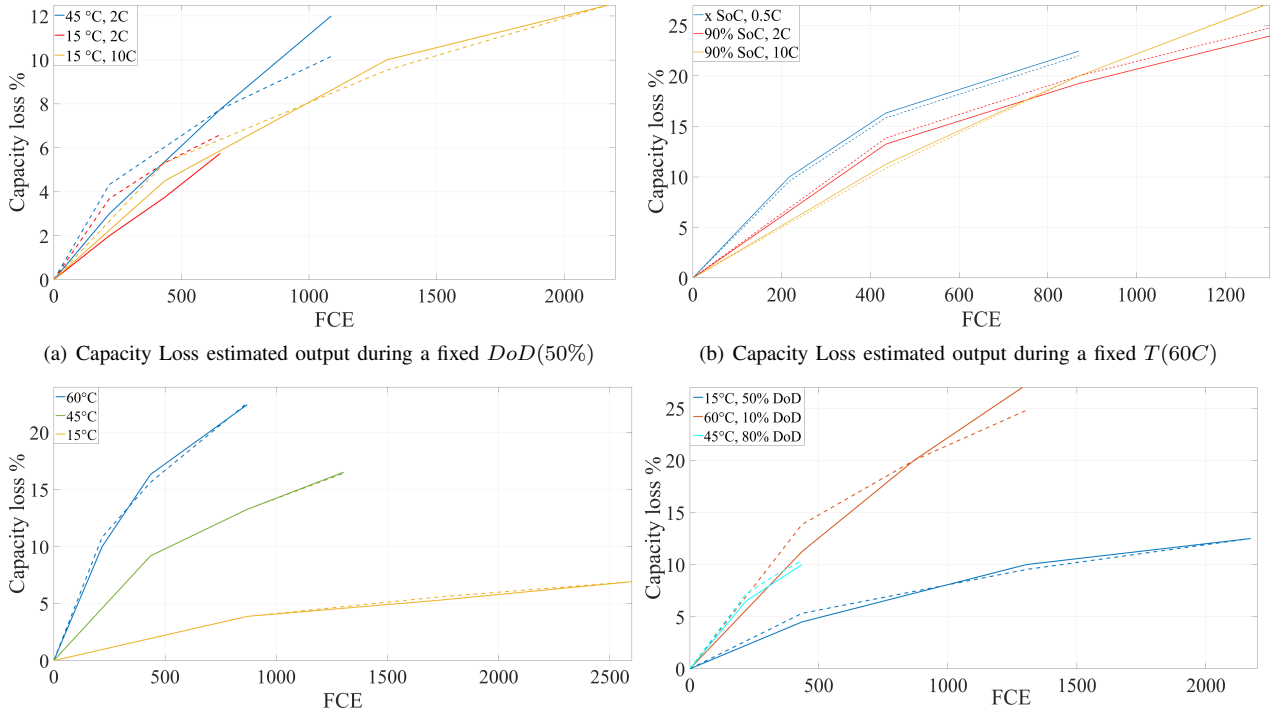

(a) Capacity Loss estimated output during a fixed $DoD(50\%)$

(b) Capacity Loss estimated output during a fixed $T(60C)$

(c) Capacity Loss estimated output during a fixed $C-rate(0.5C)$

(d) Capacity Loss estimated output during a fixed $C-rate(10C)$

Figure 7: LFP Estimated Capacity Loss during Cycling Aging.

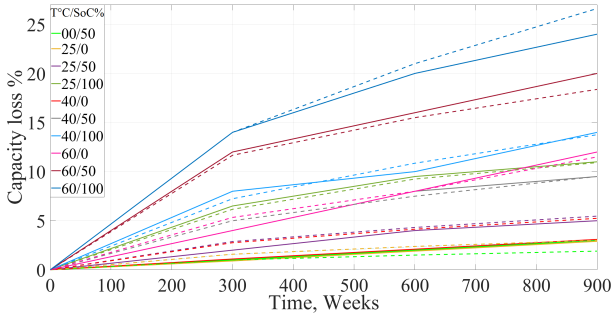

Figure 8: LFP Estimated Capacity Loss during Calendar Aging.

2011). In his work, he measured the C_{loss} during Cycling Aging in the following conditions; five different temperatures (0, 15, 25, 45, 60 °C), four levels of DOD (90%, 80%, 50%, and 10%), and four discharges rates (C/2, 2C, 6C and 10C). During discharge rate of C/2, the authors results showed that at such low rate, only temperature and FCE does have an effect on the C_{loss}, while DoD has a negligible effect on it. For the Calendar Aging C_{loss}, measured data was acquired from (Naumann et al., 2018), where the researchers studied the effect of different storage temperatures at the storage SoC = 0%,50%, and 100%.

Afterwards, the fitting process for the Cycling Aging is carried on. Similar to the LTO chemistry, the fitting process is proceed in four different scenarios; During a fixed $DoD(50\%)$, fixed temperature (60°C), and Fixed C-rate (0.5C and 10C). Figure 7 shows the estimated C_{loss} (dashed line) compared to the measured one (solid line). The average error is found to be 0.43% at half the FCE for each point, and 0.54% at the total FCE.

During the Calendar Aging process, the model has an average error of 0.45% at 450 days between the estimated C_{loss} (dashed line) and the measured one (solid line), and 0.67% at 900 days.

From the literature, it can be concluded that during Calendar Aging, the LFP chemistry degradation rate remains constant with SoC at given T, which means the C_{loss} is affected more by T and for the Cycling Aging, the C_{loss} is strongly affect by T and t on the LFP chemistry, while the DoD has almost a negligible effect especially at low C-rate (0.5C). In contrast,

Model Validation

In this section, the model is validated by comparing the estimated C_{loss} output to other known measured C_{loss}. For Cycling Aging, data needed to estimate the C_{loss} and compare it to a measured one is obtained from (Marongiu et al., 2015). Table 4, first column shows a summary of the data that used to estimate the Cycling Aging C_{loss}. The value of the battery temperature is kept at 30°C, and FCE is ranged from 1700 up to 5000.

As can been seen in Table 4, the model estimated C_{loss} error ranges from 1.2% to 1.8%, with an average error of 1.15%.

To validate the model in Calendar Aging, the same method for obtaining the required data as been used with LTO is used, and data is extracted from (Dubarry et al., 2018) . Table 5 shows a summary of the extracted data from this reference and the calculated error between the estimated C_{loss} during Calendar Aging and the measured one. The model does have an average error of 1.83% in Calendar Aging.

Table 4: Data validation during Cycling Aging measured in 30°C

Data cycling measured in 30°C	Measured Capacity Loss %	Estimated Capacity Loss %	Error %
SoC=90%, 1C	19.7	18.5	1.2
SoC=50%, 1C	17.3	18.5	1.2
SoC=20%, 1C	6.2	7.6	1.4
SoC=90%, 3C	36.6	34.9	1.7
SoC=50%, 3C	27.9	26.6	1.3
SoC=20%, 3C	56.3	54.5	1.8
SoC=90%, 6C	15.1	13.8	1.3
SoC=50%, 6C	68.1	66.7	1.4
SoC=20%, 6C	38.6	37.1	1.5

Table 5: Data validation during Calendar Aging

Temperature°C	SoC %	Capacity Loss (%/month)	Error %
0	50	0.40	0.5
10	50	0.52	0.6
20	100	1.37	1.1
25	40	1.30	1.4
30	65	0.97	2.1
40	30	1.79	1.5
45	100	3.72	2.3
50	20	3.19	4.1
60	0	1.78	2.9

Application example

After presenting, identifying and validating the battery capacity degradation model using two different types of LIBs, an attempt to predict the capacity degradation using simulated duty cycle data for a *Mining Dumper* based on (Immonen, 2003) work, is carried out. In this example, both LTO and LFP batteries are assumed to follow the same duty cycle, given in Figure 9 for Cycling Aging estimation, followed by 2 hours rest time during which the battery is cooled to the initial temperature (linear temperature decay) for the Calendar Aging estimation.

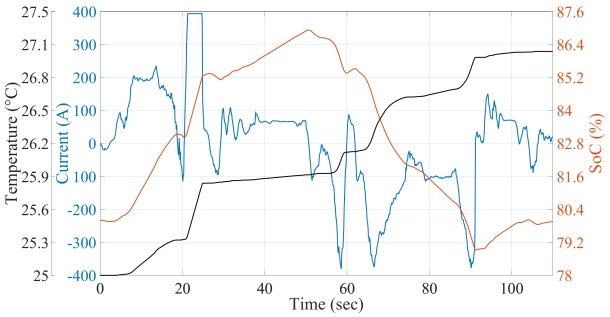

Figure 9: Simulated battery duty cycle data of a Mining Dumper.

The battery system was simulated for 1000 repeated duty and rest cycles (described above) for both LTO and LFP chemistries. The required data for predicting the capacity loss, found in Figure 9, was then fed to the proposed SEM. The results show that, for the LFP chemistry, $C_{loss}^{cyc} = 3.1\%$, and $C_{loss}^{cal} = 8.31\%$. On the other hand, for the LTO chemistry, $C_{loss}^{cyc} = 5.2\%$ and $C_{loss}^{cal} = 2.22\%$, indicating a clear difference in the aging profiles of the two battery chemistries.

CONCLUSIONS

In this work, a SEM for estimating the C_{loss} of different LIBs during Cycling Calendar Aging for different operation condition has been developed. For modeling, different LIB measurement data is required for obtaining the models' fitting parameters. Afterwards, the model is validated by comparing the estimated C_{loss} to a known one. Results show that the proposed model is able to estimate the C_{loss} during Cycling and Calendar Aging of two different LIBs (namely LTO and LFP chemistries) with a high accuracy with a brief explanation of the effect of different parameters on the two LIBs. Furthermore, a simulated battery duty cycle of a Mining Dumper has been used to estimate the C_{loss} during Cycling and Calendar Aging of a Mining Dumper.

The proposed model can be used in case of the lack of the experimental data, where it can give out an acceptable accuracy while having low computation complexity and is simpler to implement in comparison to other model-based approaches. For instance, the developed SEM has an average error of 2% between the measured C_{loss} and the estimated C_{loss}, while the adaptive-models do usually have an average error less than 1%.

In the future, the proposed SEM framework should be validated by studying different battery chemistries. Another important topic left for future work is design optimization — optimal cell chemistry selection in par-

ticular — for HDBEVs, based on the proposed battery degradation models.

REFERENCES

Andre, D., Nuhic, A., Soczka-Guth, T., & Sauer, D. (2013, mar). "comparative study of a structured neural network and an extended kalman filter for state of health determination of lithium-ion batteries in hybrid electric vehicles". *Engineering Applications of Artificial Intelligence*, *26*(3), 951–961.

Baure, G., & Dubarry, M. (2020). "battery durability and reliability under electric utility grid operations: 20-year forecast under different grid applications". *Journal of Energy Storage*, *29*, 101391.

Berecibar, M., Garmendia, M., Gandiaga, I., Crego, J., & Villarreal, I. (2016). "state of health estimation algorithm of lifepo4 battery packs based on differential voltage curves for battery management system application". *Energy*, *103*, 784–796.

Bocca, A., Sassone, A., Shin, D., Macii, A., Macii, E., & Poncino, M. (2015). A temperature-aware battery cycle life model for different battery chemistries. In *Ifip/ieee international conference on very large scale integration-system on a chip* (pp. 109–130).

Cacciato, M., Nobile, G., Scarcella, G., & Scelba, G. (2016). Real-time model-based estimation of soc and soh for energy storage systems. *IEEE Transactions on Power Electronics*, *32*(1), 794–803.

Cen, Z., & Kubiak, P. (2020). Lithium-ion battery soc/soh adaptive estimation via simplified single particle model. *International Journal of Energy Research*, *44*(15), 12444–12459.

Dubarry, M., & Devie, A. (2018). "battery durability and reliability under electric utility grid operations: Representative usage aging and calendar aging". *Journal of Energy Storage*, *18*, 185–195.

Dubarry, M., Qin, N., & Brooker, P. (2018). "calendar aging of commercial li-ion cells of different chemistries–a review". *Current Opinion in Electrochemistry*, *9*, 106–113.

Grolleau, S., Delaille, A., Gualous, H., Gyan, P., Revel, R., Bernard, J., ... Network, S. (2014). Calendar aging of commercial graphite/lifepo4 cell–predicting capacity fade under time dependent storage conditions. *Journal of Power Sources*, *255*, 450–458.

Immonen, P. (2003). *Energy efficiency of a diesel-electric mobile working machine* (Unpublished doctoral dissertation). Lappeenranta University of Technology.

Kluschke, P., Gnann, T., Plötz, P., & Wietschel, M. (2019). "market diffusion of alternative fuels and powertrains in heavy-duty vehicles: A literature review". *Energy Reports*, *5*, 1010–1024.

Lagarias, J. C., Reeds, J. A., Wright, M. H., & Wright, P. E. (1998). Convergence properties of the nelder–mead simplex method in low dimensions. *SIAM Journal on optimization*, *9*(1), 112–147.

Liimatainen, H., van Vliet, O., & Aplyn, D. (2019). "the potential of electric trucks–an international commodity-level analysis". *Applied energy*, *236*, 804–814.

Liu, Z., Zhao, J., Wang, H., & Yang, C. (2020). "a new lithium-ion battery soh estimation method based on an indirect enhanced health indicator and support vector regression in phms". *Energies*, *13*(4), 830.

Marongiu, A., Roscher, M., & Sauer, D. U. (2015). "influence of the vehicle-to-grid strategy on the aging behavior of lithium battery electric vehicles". *Applied Energy*, *137*, 899–912.

Naha, A., Han, S., Agarwal, S., Guha, A., Khandelwal, A., Tagade, P., ... Oh, B. (2020, dec). "an incremental voltage difference based technique for online state of health estimation of li-ion batteries". *Scientific Reports*, *10*(1), 9526.

Naumann, M., Schimpe, M., Keil, P., Hesse, H. C., & Jossen, A. (2018). "analysis and modeling of calendar aging of a commercial lifepo4/graphite cell". *Journal of Energy Storage*, *17*, 153–169.

Petit, M., Prada, E., & Sauvant-Moynot, V. (2016, jun). Development of an empirical aging model for Li-ion batteries and application to assess the impact of Vehicle-to-Grid strategies on battery lifetime. *Applied Energy*, *172*, 398–407. doi: 10.1016/j.apenergy.2016.03.119

Schmalstieg, J., Käbitz, S., Ecker, M., & Sauer, D. U. (2014, jul). A holistic aging model for Li(NiMnCo)O2 based 18650 lithium-ion batteries. *Journal of Power Sources*, *257*, 325–334. doi: 10.1016/j.jpowsour.2014.02.012

Singh, P., Chen, C., Tan, C. M., & Huang, S.-C. (2019). Semi-empirical capacity fading model for soh estimation of li-ion batteries. *Applied Sciences*, *9*(15), 3012.

Standard practices for cycle counting in fatigue analysis (Standard). (2005). West Conshohocken, PA, USA: ASTM International.

Wang, J., Liu, P., Hicks-Garner, J., Sherman, E., Soukiazian, S., Verbrugge, M., ... Finamore, P. (2011). "cycle-life model for graphite-lifepo4 cells". *Journal of power sources*, *196*(8), 3942–3948.

Yang, K., Chen, Z., He, Z., Wang, Y., & Zhou, Z. (2020). "online estimation of state of health for the airborne li-ion battery using adaptive dekf-based fuzzy inference system". *Soft Computing*, *24*(24), 18661–18670.

AUTHOR BIOGRAPHIES

Mohammed Rabah PhD, is a Research Engineer at Computational Engineering and Analysis (COMEA) research group, Turku University of Applied Sciences, Finland.
E-mail:mohamed.rabah@turkuamk.fi

Eero Immonen D.Sc. (Tech.) and Adjunct Professor, leader of the Computational Engineering and Analysis (COMEA) research group at Turku University of Applied Sciences, Finland.
E-mail:eero.immonen@turkuamk.fi

Sajad Shahsavari works as Researcher at Turku University of Applied Sciences, and is a PhD student at University of Turku, Finland.
E-mail:sajad.shahsavari@turkuamk.fi

Mohammad-Hashem Haghbayan is a Post-Doctoral Researcher at Department of Future Technologies, University of Turku, Finland.
E-mail:mohammadhashem.haghbayan@utu.fi

Kirill Murashko PhD (M), is a Post-Doctoral Researcher at Department of Environmental and Biologic Science, University of Eastern Finland, Finland.
E-mail:kirill.murashko@uef.fi

Paula Immonen D.Sc. (Tech.) and Associate Professor of the School of Energy Systems, LUT University, Finland.
E-mail:paula.immonen@lut.fi